HHS Public Access

Author manuscript

Oncogene. Author manuscript; available in PMC 2020 March 10.

Published in final edited form as:

Oncogene. 2018 August ; 37(32): 4428–4442. doi:10.1038/s41388-018-0263-7.

Fibroblast-Derived CXCL12 Promotes Breast Cancer Metastasis by Facilitating Tumor Cell Intravasation

Dinesh K. Ahirwar[1], **Mohd W. Nasser**[1], **Madhu M. Ouseph**[2], **Mohamad Elbaz**[1], **Maria C. Cuitiño**[2], **Raleigh D. Kladney**[2,5], **Sanjay Varikuti**[1], **Kirti Kaul**[1], **Abhay R. Satoskar**[1], **Bhuvaneswari Ramaswamy**[3,5], **Xiaoli Zhang**[4], **Michael C. Ostrowski**[2,5], **Gustavo Leone**[2,5,*,†], **Ramesh K. Ganju**[1,5,*,†]

[1]Department of Pathology; Ohio State University, Columbus, OH 43210

[2]Department of Cancer Biology and Genetics; Ohio State University, Columbus, OH 43210

[3]Department of Internal Medicine; Ohio State University, Columbus, OH 43210

[4]Center for Biostatistics; Ohio State University, Columbus, OH 43210

[5]Comprehensive Cancer Center; Ohio State University, Columbus, OH 43210

Abstract

The chemokine CXCL12 has been shown to regulate breast tumor growth, however, its mechanism in initiating distant metastasis is not well understood. Here, we generated a novel conditional allele of *Cxcl12* in mice and used a fibroblast-specific *Cre* transgene along with various mammary tumor models to evaluate CXCL12 function in the breast cancer metastasis. Ablation of CXCL12 in stromal fibroblasts of mice significantly delayed the time to tumor onset and inhibited distant metastasis in different mouse models. Elucidation of mechanisms using *in-vitro* and *in vivo* model systems revealed that CXCL12 enhances tumor cell intravasation by increasing vascular permeability and expansion of a leaky tumor vasculature. Furthermore, our studies revealed CXCL12 enhances permeability by recruiting endothelial precursor cells and decreasing endothelial tight junction and adherence junction proteins. High expression of stromal CXCL12 in large cohort of breast cancer patients was directly co-related to blood vessel density and inversely co-related to recurrence and overall patient survival. In addition, our analysis revealed that stromal CXCL12 levels in combination with number of CD31+ blood vessels have poorer patient survival compared to individual protein level. However, no co-relation was observed between epithelial CXCL12 and patient survival or blood vessel density. Our findings describe the novel interactions between fibroblasts-derived CXCL12 and endothelial cells for facilitating tumor cell intrvasation, leading to distant metastasis. Overall, our studies indicate that cross-talk between fibroblast–

*Correspondence to: ramesh.ganju@osumc.edu or gustavo.leone@osumc.edu.
†The authors contributed equally

AUTHOR CONTRIBUTIONS

DKA, WMN, MMO, GL and RKG designed the experiments. All authors performed the experiments and collected and analyzed the data. RKG and GL supervised the studies. DKA, GL, MCO and RKG wrote the manuscript with inputs from all the authors.

CONFLICT OF INTEREST

We have no competing financial interests or any conflict of interest to disclose.

derived CXCL12 and endothelial cells could be used as novel biomarker and strategy for developing tumor microenvironment based therapies against aggressive and metastatic breast cancer.

Keywords

Fibroblasts; CXCL12; Metastasis; Intravasation; Endothelial cells; Breast Cancer

INTRODUCTION

Bi-directional communication between mesenchymal and epithelial cells is critical for development of multi-cellular organisms.[1] Coordinated signaling between different cell types is also a necessary response to extreme but physiological stresses such as wounding, infection or pregnancy.[2] However, inappropriate inter-cellular signaling may also contribute to disease, including auto-immune disorders, neuro-degeneration and cancer.[1, 2] In epithelial cancers, stromal cells (fibroblasts, endothelial cells, adipocytes and immune cells) are activated to modulate extra-cellular matrix components and activities that foster epithelial cell transformation, tumor initiation, progression and the escape of cancer cells from the primary tumor site to distant organ sites.[3] Metastasis is a major clinical challenge responsible for most cancer related mortalities.[4] Chemokine (C-X-C motif) ligand 12 (CXCL12) is a secreted factor present in tumor microenvironment believed to be one of the major players in facilitating cancer growth.[5] Breast cancer cells express high level of C-X-C chemokine receptor type 4 (CXCR4) and migrate to the organs expressing high levels of its ligand CXCL12.[6] However, it is not clear if the CXCL12 present in primary tumor microenvironment or CXCL12 present in distant organs regulate metastasis. Furthermore, the role of CXCL12 in regulating various stages of metastasis has also not been studied yet.

Cancer associated fibroblasts (CAFs) are a principal constituent of the tumor microenvironment that express and secrete a myriad of growth factors, chemokines and structural as well as enzymatic components of the extra-cellular matrix. These secretomes can directly engage tumor cells, but can also reprogram other cell types in the tumor microenvironment, including macrophages, immune cells and endothelial cells to indirectly impact tumor cell invasion and metastasis.[7] However, the role of fibroblasts-derived CXCL12 in regulating the functions of other stromal cells in TME is not known. To further, analyze the role of CXCL12 in TME and its mechanism in regulating metastasis, we generated a conditional allele of *Cxcl12* (*Cxcl12*^{f}) and used the *Fsp-cre* transgene to specifically ablate CXCL12 in stromal fibroblasts and asses breast cancer growth and metastasis using different *in vitro* and *in vivo* models. Fibroblast-specific ablation of CXCL12 suppressed tumor growth and abolished distant metastasis. Mechanistically, fibroblast-derived CXCL12 facilitated tumor cell intravasation by increasing blood vessel leakiness through weakening endothelial tight junctions. Importantly, increased levels of CXCL12 in stromal fibroblasts of human breast cancers correlated with higher vascular density, increased recurrence and decreased overall patient survival. Thus, these studies implicate the novel role of CAF-derived CXCL12 in modulating tumor microenvironment by targeting endothelial cells to promote breast cancer metastasis.

RESULTS

CXCL12 is essential for embryonic viability

To rigorously investigate the role of CXCL12 *in vivo*, we utilized homologous recombination and *LoxP*-cre technology to conditionally disable *Cxcl12* in mice. The targeting vector contains an *Frt*-flanked Neomycin selection cassette, *LoxP* sites on either side of exons 1 and 2 and a herpes simplex virus thymidine kinase negative selection cassette (Figure 1A). The targeting vector was electroporated into ES cells and positive clones were selected by Southern blotting (Supplementary Figure S1). Targeted ES cells were injected into pseudo-pregnant females and the resulting founder offspring were bred with wild type mice to yield germ-line transmission of the targeted allele. *Flp* mediated recombination of the *Frt*-flanked neomycin cassette resulted in deletion of the Neo-cassette and generation of the conditional floxed allele ($Cxcl12^{f}$). Interbreeding *Sox2-Cre* with $Cxcl12^{f/f}$ mice generated heterozygous offspring lacking the *LoxP*-flanked region ($Cxcl12^{-/+}$). All alleles were identified by Southern Blot and PCR genotyping (Figure. 1B and; Supplementary Figure S1 B–E). Ablation of *Cxcl12* expression was confirmed by quantitative real time PCR (qRT-PCR; Figure 1C). Intercrosses between $Cxcl12^{-/+}$ mice resulted in 50% fewer $Cxcl12^{-/-}$ newborn pups (P0) than expected and those that were alive died within 2 days (P2) of birth (Figure 1D). Timed pregnancies between $Cxcl12^{-/+}$ mice resulted in the expected ratios of E14.5 embryos, albeit 50% of the $Cxcl12^{-/-}$ embryos were smaller than litter mate controls and exhibited significant hemorrhaging (Figure. 1E). Consistent with a previously generated null *Cxcl12* allele,[8] these observations suggested that global *Cxcl12* deficiency compromises embryonic growth, vascular integrity and perinatal lethality.

Stromal CXCL12 enhances tumor growth and metastasis

We then used a mesenchymal-specific *Fsp-cre* mouse generated by our laboratory[9] to evaluate the role of fibroblast-derived CXCL12 in mammary tumorigenesis using the well-established Polyoma middle T antigen (*PyT*) mammary tumor model.[10] In the mammary gland, *Fsp-cre* expression is restricted to stromal fibroblasts surrounding epithelial ducts, and is not expressed in leukocytes, myeloid cells or other mammary stromal cell types.[11] Fibroblast specific deletion of *Cxcl12* did not induce perinatal lethality and control ($Cxcl12^{f/f}$) and *Fsp-cre;*$Cxcl12^{f/f}$ ($Cxcl12^{\Delta/\Delta}$) females were viable, had normal external appearance and were fertile (Supplementary Figure S2). Efficient fibroblast-specific ablation of CXCL12 was confirmed by western blot analysis of isolated fibroblasts (Figure 2A) and by immunofluorescence (IF) of sections prepared from mammary gland (Figure 2B). Macrophages in PyT tumors have been shown to express FSP and therefore, may affect CXCL12 expression in $Cxcl12^{\Delta/\Delta}$*;PyT* tumors.[12] IHC analysis demonstrated expression of CXCL12 on tumor and stromal cells that was absent in F4/80 positive macrophages in PyT tumors (Supplementary Figure S3 A–B). In addition, Cxcl12 RNA hybridization revealed that CXCL12 is expressed by platelet-derived growth factor receptor-alpha (PDGFR-α) positive stromal fibroblasts but not by tumor cells or F4/80 positive macrophages present in PyT tumors (Figure 2 C–D and Supplementary Figure S3 C–D). qRT PCR analysis of Cxcl12 expression in fibroblasts (CD3-/CD90.1+ cells) and macrophages (CD11b+/F4/80+ cells) isolated from *f/f;PyT* tumors confirmed fibroblasts-specific origin of CXCL12

expression (Supplementary Figure S3E). Cohorts of control (*Cxcl12$^{f/f}$;PyT*) or *Fsp-cre;Cxcl12$^{f/f}$;PyT* (*Cxcl12$^{\Delta/\Delta}$;PyT*) females were evaluated over a period of three months. Deletion of *Cxcl12* in stromal fibroblasts significantly delayed tumor onset (Figure 3A) and reduced tumor burden (Figure 3B; Supplementary Figure S4A). While apoptotic rates were similar among the two groups, tumor cell proliferation, as measured by Ki67 IHC, was reduced in *Cxcl12* stromal-deleted tumors compared to controls (Supplementary Figure S4 B–E). We then measured circulating tumor cells and lung metastasis in mice with equal primary tumor burden. Quantitative RT-PCR of total blood RNA showed decreased levels of circulating *PyT* mRNA in *Cxcl12$^{\Delta/\Delta}$;PyT* females, suggesting decreased number of tumor cells in the circulation (Figure 3C). Inspection of lungs and pathological evaluation of H&E stained lung sections revealed that *Cxcl12$^{\Delta/\Delta}$;PyT* females had very few metastatic tumors compared to control *Cxcl12$^{f/f}$;PyT* mice (Figure 3 D–E; Supplementary Figure S5). Thus, *Cxcl12* deficiency in stromal fibroblasts resulted in reduced tumor initiation and metastatic progression.

Metastasis to distant organs involves two major steps, local invasion and intravasation into the tumor vasculature, followed by extravasation and colonization into the metastatic niche. To discriminate between these two steps in the metastatic process, we first used an orthotopic MVT1 tumor model. The MVT1 mammary tumor cells over-expressing the VEGF and c-MYC oncogenes[13] were orthotopically implanted into the mammary fat pad of *Cxcl12$^{f/f}$* or *Cxcl12$^{\Delta/\Delta}$* syngeneic mice and lung metastasis was evaluated over a period of 45 days (Figure 3F). Tumor growth rate was identical between both the groups (Supplementary Figure S6 A–B). However, the number of metastatic lung nodules was dramatically reduced in *Cxcl12$^{\Delta/\Delta}$* mice compared to controls (Fig. 3 G–H). This was confirmed by H&E staining of lung sections (Supplementary Figure S6 C–D). These observations suggested a direct role of fibroblast-derived CXCL12 in metastasis that is independent of primary tumor burden.

We also injected MVT-1 cells into the peripheral vasculature of control or *Cxcl12$^{\Delta/\Delta}$* syngeneic mice via the tail vein and evaluated their colonization in lungs after two weeks (Figure 3I and; Supplementary Figure S7A). H&E stained sections showed that tumor cells colonized the lungs of control and *Cxcl12$^{\Delta/\Delta}$* mice equally well (Figure 3J and; Supplementary Figure S7B). Next, we evaluated the role of fibroblasts-derived CXCL12 in tumor cell migration and invasiveness. By using transwell migration and invasion assays, we observed that fibroblasts-derived CXCL12 increases the migratory and invasive potential of tumor cells (Figure 4 A–C). All together, these results suggested that fibroblast-derived CXCL12 promotes early events in the metastatic process by increasing the invasion and intravasation of tumor cells at the primary site into the surrounding vasculature.

Fibroblast-derived CXCL12 facilitates tumor cell intravasation through hyper-permeable vasculature

Metastasis is associated with increased angiogenesis and vasculature permeability. Thus, we evaluated the tumor microvasculature by immunohistochemistry using the endothelial-specific marker CD31. This analysis revealed decreased CD31+ve blood vessels in *Cxcl12$^{\Delta/\Delta}$;PyT* relative to control *PyT* tumors (Figure 5 A–B). We also found a significantly

increased number of blood vessels in orthotopic syngeneic control *Cxcl12*$^{f/f}$*-MVT-1* tumors compared to fibroblast-CXCL12 depleted *Cxcl12*$^{\Delta/\Delta}$-MVT1 tumors (Supplementary Figure S8). The effect of CAFs-derived CXCL12 on angiogenesis was directly measured *in vitro* by using tube formation assay. The tube formation ability of mouse embryonic endothelial cells (MEECs) was significantly increased by addition of conditioned media (CM) from wild type CAFs compared to CM from CXCL12 depleted CAFs, which was reversed by adding recombinant CXCL12. Furthermore wild type CAFs induced tube formation was inhibited by CXCR4 receptor inhibitor AMD3100 (Supplementary Figure S9A–B). Neo-angiogenesis is mediated, in part, by the recruitment of CD31$^+$/Sca1$^+$ endothelial precursor cells (EPCs) into pre-existing blood vessels.[14, 15] Flow cytometry of single cell suspensions showed that *Cxcl12*$^{\Delta/\Delta}$*;PyT* tumors had fewer CD31$^+$/Sca1$^+$ EPCs than control *PyT* tumors (Figure 5C and; Supplementary Figure S9C), suggesting a role for fibroblast-secreted CXCL12 in the recruitment of EPCs into the tumor microenvironment.

We then analyzed tumor blood vessel integrity by injecting high molecular weight fluorescently labeled FITC-dextran (F-dextran) and visualizing its diffusion into the tumor tissue. Control *PyT* tumors displayed a chaotic, torturous vascular architecture, with extensive dilation and leakiness. In contrast, blood vessels in *Cxcl12*$^{\Delta/\Delta}$*;PyT* tumors had the typical structural hierarchy of primary and secondary vessels found in normal tissues (Figure 5 D–E and; Supplementary Figure S9D). Moreover, we observed a better retention of F-dextran within blood vessels of females with stromal *Cxcl12* deficiency (Figure 5D, side panels), suggesting improved vascular integrity.

Vascular permeability of endothelial cells was directly measured *in vitro* using a tumor cells and fibroblasts co-culture transwell migration assays. The migration of Carboxyfluorescein succinimidyl ester (CFSC) tagged MVT-1 cells across endothelial cells layer was calculated as a measure of transendothelial migration ability. Transendothelial migration of tumor cells was significantly increased when MEECs were co-cultured with wild type CAFs compared to CXCL12 depleted CAFs. Furthermore, CXCR4 receptor inhibitor, AMD-3100 inhibited wild type CAFs induced transendothelial migration of tumor cells. (Figure 5F and; Supplementary Figure S9E). In addition, reduced transedothelial migration of tumor cells in the presence of CXCL12-depleted CAFs was restored upon addition of recombinant CXCL12 (Figure 5F and; Supplementary Figure S9E). We further analyzed the effect of CAFs-derived CXCL12 on endothelial cell permeability by using high molecular weight, fluorescently conjugated Dextran (FITC-Dextran) and transwell permeability assay (Supplementary Figure S9F). Diffusion of F-dextran across the endothelial cell layer was significantly increased when MEECs were co-cultured with control CAFs. This increase was dampened when mouse embryonic endothelial cells (MEECs) were co-cultured with CXCL12-depleted CAFs (Supplementary Figure S9G). These results strongly suggest the direct role of fibroblasts-derived CXCL12 in enhancing the permeability of endothelial cells through CXCR4 receptor.

Tight junction molecules ZO-1, Occludin-1 and adherence junction molecule VE-Cadherin control the permeability of blood vessels.[16, 17] Thus, we next evaluated whether CXCL12-depleted fibroblasts affected the composition of endothelial tight junctions. Flow cytometry of single cell suspensions from tumors showed an increase in the number of VE-Cadherin$^+$/

CD31$^+$ and Occludin-1$^+$/CD31$^+$ cells in *Cxcl12$^{\Delta/\Delta}$;PyT* than in *Cxcl12$^{f/f}$;PyT* females (Figure 6 A–D). IF showed lower levels of ZO-1 in CD31$^+$ endothelial cells in *Cxcl12$^{\Delta/\Delta}$;PyT* than in either *Cxcl12$^{f/f}$;PyT* tumors or normal *Cxcl12$^{f/f}$* mammary glands (Figure 6E). Together, these findings strongly suggested that inactivation of *Cxcl12* from stromal fibroblasts restored normal vascular structure and function in tumors by reducing aberrant neo-angiogenesis and stabilizing endothelial tight junctions.

Stromal fibroblast CXCL12 expression predicts patient survival

To determine the clinical relevance of our findings, we initially compared the mRNA expression of *CXCL12* from published laser-captured microdissected (LCM) tumor stroma (53 samples) and normal stroma (6 samples) in human patients with breast cancer (GEO; GSE9014).[18] This analysis revealed a significantly higher level of *CXCL12* expression in tumor stroma than in normal stroma (18.556 fold change, p=6.99e-21; Figure 7A). We then used IHC to assess the expression of CXCL12 protein in tumors and adjacent normal tissue of breast cancer patients treated at the OSU Spielman Breast Cancer Center (SBCC). Analysis of a tissue microarray (TMA; 267 breast cancer patients of all subtypes) by a licensed pathologist showed high levels of CXCL12 protein in CAFs compared to normal fibroblasts or fibroblasts in non-malignant lesions (Figure 7B). The levels of stromal CXCL12 varied among patient samples across all subtypes. High CXCL12 levels imposed greater risk for advanced stage and grade, irrespective of molecular subtype (Supplementary Figure S10A). Further, we found that high CXCL12 expression levels predicted reduced overall survival (OS) and recurrence free survival (RFS) across all subtypes of breast cancer patients (Figure 7 C–D). In contrast, high levels of CXCL12 present in the tumor epithelium compartment failed to predict OS or RFS (Supplementary Figure S10 B–D).

Given our observation connecting CXCL12 to neo-angiogenesis and vascular function, and previous work showing that blood vessel density is an independent prognostic marker of breast cancer,[19, 20] we also measured blood vessel density in the SBCC patient cohort. IHC with CD31-specific antibody showed that high blood vessel density was inversely correlated with improved OS and RFS (Supplementary Figure S11 A–B) as previously reported.[19, 20] Moreover, increased blood vessel density was correlated with high levels of CXCL12 protein in stromal fibroblasts of breast cancer patients (Supplementary Figure S11 C–D). Importantly, Kaplan-Meier plots revealed that patients with high expression of CXCL12 and blood vessel density had the shortest RFS and worse OS (Figure 7 E–F and; Supplementary Figure S11 E–F). In summary, these observations establish a critical role for CXCL12 made by stromal fibroblasts in promoting breast cancer growth and metastasis.

DISCUSSION

Although CXCL12 present at secondary organs has been proposed to chemoattract CXCR4-positive cancer cells and facilitate metastasis, the role of CXCL12 present in primary TME on different stages of metastasis has not been evaluated yet. In the present study, for the first time we have shown that the deletion of CXCL12, specifically from cancer associated fibroblasts within the TME prevents cancer cell intravasation, thereby significantly inhibiting spontaneous mammary tumor metastasis to the lungs.

We have generated a conditional allele of CXCL12 to study the role of carcinoma associated fibroblasts-derived CXCL12 in metastasis. We show that mice with fibroblast-specific deletion of *Cxcl12* are born and develop to adulthood, whereas the global knockout of CXCL12 leads to extensive hemorrhaging and perinatal lethality. Others have also shown that the mice lacking CXCL12 or its receptor CXCR4 die perinatally due to hemorrhaging, cardiac ventricular septal and arterial defects.[8, 21–24]

In addition to their function in development and maintenance of healthy organs, we defined a critical role for CXCL12 made in fibroblasts in promoting tumor onset and growth. Mechanistic studies showed that depleting fibroblast-derived CXCL12 inhibits proliferation of tumor cell and EPCs recruitment to the TME that expands the tumor vasculature. However, we did not observe any difference in growth of orthotopic syngeneic tumors that are depleted for fibroblast-CXCL12 compared to control tumors. MMTV-PyMT tumors undergo initial stages of tumor development, whereas, aggressive tumors were implanted in orthotopic syngeneic tumor model, which suggests that CXCL12 is required for initial stages of tumor initiation. Secreted CXCL12 has been implicated in trafficking and engraftment of CXCR4-positive EPCs to the site of angiogenesis.[21, 25] However, fibroblast-secreted CXCL12 compromised the integrity of this expanded vasculature by increasing the permeability. By using an *in vitro* endothelial cell permeability assay, we found that CAFs can increase the permeability of endothelial cells layer in CXCL12 specific manner. Using *in vivo* models, we confirm that the tumor induced vasculature hyper-permeability can be reversed by depleting CXCL12 from CAFs. We have observed that the tumor bearing mice lacking fibroblast-derived CXCL12 have significantly reduced number of circulatory tumor cells (CTCs). Of note, a recent finding showed a direct correlation between CXCL12 present in tumors and circulatory tumor cell markers in peripheral blood of breast cancer patients, indicating high stromal CXCL12 may facilitate tumor cell intravasation to peripheral blood.[26]

Consequently, CXCL12 mediated enhanced tumor vasculature permeability and tumor cell intravasation promoted cancer cell dissemination into the systemic circulation, facilitating colonization to distant organs. The process of metastasis involves different steps including tumor cells basement membrane invasion and intravasation in to the circulation and colonization to distant organs. Using various *in vivo* models, we for the first time, demonstrated that fibroblast derived CXCL12 facilitate tumor cell intravasation and thereby enhances metastasis to the lungs. We further established that CXCL12 acts on endothelial cells through CXCR4 and promote trans-endothelial migration of tumor cells. Further elucidation of mechanisms that regulate CXCL12-mediated vascular hyperpermeability revealed that CAFs-derived CXCL12 reduces the expression of key endothelial cell tight junction and adherence junction molecules such as ZO-1, occludin-1 and VE-Cadherin.[27] A recent study indicates that CXCL12 produced by stromal cells in response to TGF-β can prevent metastasis. This contradictory finding could be due to the use of orhotopic syngeneic tumor model and also analyzing the effect of TGF-β on CXCL12-regulated metastasis in that study.[28] However, in our study we have used a spontaneous transgenic tumor model in which the CXCL12 is depleted in fibroblasts. The role of fibroblasts-specific CXCL12 in promoting breast cancer growth and angiogenesis has been shown before in breast cancer xenograft mouse model.[5] However, its role in distant metastasis and tumor cell intravasation

has not been studied yet. By using a novel Cxcl12 conditional allele, FSP-Cre transgene, and spontaneous MMTV-PyMT tumor model, we clearly show that the fibroblasts derived CXCL12 is critical for enhanced endothelial permeability, tumor cell intravasation and metastasis to the lungs.

These findings have a potentially profound translational impact since we observed a direct link between CXCL12 levels in tumor associated fibroblasts and blood vessel density, and an inverse relationship with breast cancer patient survival. Importantly, we found this CXCL12-angiogenic axis to be associated with poorer overall and disease free survival in human patients across all major breast cancer subtypes. Despite strong CXCL12 expression in tumor epithelial cells, we failed to observe any correlation between CXCL12 in tumor epithelial cells and patient survival, suggesting that the source of CXCL12 is a key determinant of metastatic potential. The RNA expression analysis clearly demonstrated that only fibroblasts express CXCL12. However, the paradoxical localization of CXCL12 protein on tumor cell observed in immunofluorescence analysis of PyT tumors could be due to bound form of CXZCL12 to high mobility group box 1 (HMGB1). HMGB1 has been shown to form a high affinity heterocomplex with CXCL12 and is overexpressed by metabolically stressed tumor cells.[29–31] Presumably, CXCL12 made in distinct cellular compartments is either processed differently, interacts with diverse sets of proteins and/or has cell-specific functions.[31] Hence, stromal CXCL12 expression in combination with blood vessel density could be a potential biomarker to identify patients with tumors that need more aggressive therapy.

Stromal derived CXCL12 may have additional functions beyond impacting endothelial cells and tumor vasculature. In a mouse model of pancreatic cancer, CXCL12 produced by Fibroblast Activated Protein (FAP)-positive stromal cells was shown to be immune suppressive and accounted for the lack of $CD8^+$ T-cells in tumors.[31] Additionally, CXCL12 may directly affect T-cell differentiation and functions. Future studies are needed to determine whether CXCL12-dependent changes in the tumor vasculature may also indirectly contribute to an immune-suppressive microenvironment.

In summary, our findings define that the source of CXCL12 is a key determinant of tumor cell intravasation and the metastatic potential. Our studies also depict that CAFs–secreted CXCL12 as a major factor within the TME that cross-talks with endothelial cells and thereby expands a highly unstable and hyper-permeable vasculature, enabling the escape of tumor cells from the primary site to other distant organs. In addition, stromal CXCL12 along with blood vessel density could be used as better prognostic biomarkers in breast cancer patients.

METHODS

Ethics statement

Mouse experiments and usage has been approved by Institutional Animal Care and Use Committee at the Ohio State University. All clinical data were collected following approval by the Ohio State University Medical Center institutional review board.

Mice modeling and usage

Generation of Cxcl12 conditional knockout mouse model—Generation of *Cxcl12*$^{f/f}$ conditional allele is described in the Supplemental Experimental Procedures.

Transgenic tumor model—The *Cxcl12*$^{f/f}$ and *Cxcl12*$^{\Delta/\Delta}$ mice were intercrossed with Mouse Mammary Tumor Virus promoter-polyoma middle T antigen (*PyT)* (Jackson laboratories, USA) to generate *Cxcl12*$^{f/f}$;*PyT* and *Cxcl12*$^{\Delta/\Delta}$;*PyT* mice. Tumor diameter was measured externally using a digital caliper and tumor volume was calculated according to the formula V= 0.52 × a^2× b, where 'a' is the smaller and 'b' is the bigger diameter of tumor. The tumor and lungs were harvested when tumors achieved the size of 2 cm. The tumors were weighed and were normalized with the weight of mammary glands of no tumor bearing mice of similar age. Lung metastasis was analyzed histologically. Briefly, formalin-fixed paraffin embedded lung sections (3 sections per mouse spaced 200 μm apart) were stained with hematoxylin and eosin. The micro-nodules were counted or analyzed by ImageJ for pixel counts. The pixel numbers of the nodules were divided by that of the total lung area, and the average of 3 sections was obtained for each mouse.

Orthotopic tumor model—Mouse mammary tumor MVT1 cells (1×10^6) overexpressing *c-Myc* and *VEGF* were suspended in 100 μl PBS were orthotopically injected into the #4 mammary gland of *Cxcl12*$^{f/f}$ and *Cxcl12*$^{\Delta/\Delta}$ and allowed to grow up to 45 days. Tumor weight and volume was measured as described above. The animals were sacrificed and tumors and lungs were harvested at day 45.

Tail vain tumor model—The MVT1 cells (1×10^6) were injected to *Cxcl12*$^{f/f}$ and *Cxcl12*$^{\Delta/\Delta}$ through lateral tail vain as described earlier[32]. After 15 days, lungs were harvested, fixed, processed and analyzed for MVT1 metastasis histologically.

Circulatory tumor cells analysis

The heart blood was collected into EDTA Vacutainers (BD Bioscience) and the cells were pelleted by centrifugation. Red blood cells were lysed by RBC lysis buffer (BioLegend) followed by washing the cells with PBS twice. RNA was extracted by RNeasy plus mini kit (Qiagen). Total RNA was converted to cDNA by using random hexamer primers (Applied Biosystems 4368814). The PyMT gene expression was analyzed by RT-PCR (realplex^2; Eppendorf, USA) using 5′- CAGAAAGCGACCAAGACCAG-3′ and 5′-CCTCCATTGGCATGTACTCC-3′ primers.

In-Vivo blood vessel permeability assay

To visualize blood vessels and analyze their leakiness, mice were injected i.v. with 100 μl of saline containing FITC-labeled dextran (FITC-dextran, 2 ×10^6 MW, Sigma Aldrich, USA). After 30 minutes, mice were euthanized and tumor tissues were collected and fixed in 4% cold paraformaldehyde for 4 hrs. The fixed tissues were processed for confocal microscopic analysis and imaged by Olympus FV1000 confocal scanning microscope. Mean blood vessel diameter was quantified using ImageJ software (NIH, USA).

Estrous cycle staging

The mouse estrous cycle stages were identified according to the standard procedure.[33] See Supplemental Experimental Procedures for further details.

Whole-Mount Carmine staining

Mammary Glands (#4 gland) were harvested from 12 weeks old *Cxcl12*$^{f/f}$ and *Cxcl12*$^{\Delta/\Delta}$ females and spread out on glass slides. The whole mammary gland specimens were fixed in a 3:1 solution of 100% ethanol and glacial acetic acid at 4 °C overnight. The tissues were hydrated with serial solutions of 70, 50 and 30%ethanol for 15 minutes each, and rinsed with distilled water for 15 minutes. The glands were then stained with Carmine Alum (1 g Carmine, #C1022, 2.5 g Aluminium potassium sulphate, #A7167, Sigma St Louis, MO in 500 ml of water) overnight at 4°C. The tissues were rinsed in deionized water and dehydrated through graded alcohols and cleared in xylene prior to mounting with Permount mounting media (Fisher Scientific, USA).

RNA hybridization

The RNA hybridization was performed by using RNAScope Multiplex Fluorescent Reagent Kit v2 (Advanced Cell Diagnostics (ACD), USA # 323100) by following manufacturer's instructions. Briefly, 4μM sections of paraformaldehyde fixed paraffin embedded PyT tumors were deparaffinized in xylene, followed by dehydration in an ethanol series. Next, the tissue sections were incubated with H_2O_2 for 10 minutes at room temperature (RT) followed by target retrieval in target retrieval buffer (ACD #322000) maintained at a boiling temperature (100°C to 103°C) using a hot plate for 15 minutes, rinsed in deionized water, and immediately treated with protease plus (ACD # 322381) at 40°C for 30 minutes in a HybEZ hybridization oven (Advanced Cell Diagnostics, Hayward, CA). The sections were then incubated in at 40°C with the *CXCL12* and *F4/80* or *PDGFR-α* target probes for 2 hours followed by preamplifier in HybEZ hybridization oven. The fluorescent signals were developed by Opal dye system (ParkinElmer, USA). The images were captured by Zeiss LSM-700 confocal microscope.

Cell culture

The mouse embryonic endothelial cells (MEECs) were generous gift from Dr. Nam Y. Lee (The Ohio State, Ohio, USA) and were cultured in endothelial cell media supplemented with endothelial cell growth supplement, Vascular endothelial growth factor and heparin (Cell Biologics: M1168). The primary fibroblasts were isolated from mouse mammary glands (MMFs) and tumors (CAFs) as described before with minor modifications.[34] Briefly, 8 week-old female mice mammary glands were minced and digested with collagenase (0.15% Collagenase I, 160 U/ml Hyaluonidase, 1 μg/ml hydrocortisone and 10 μg/ml insulin with penicillin and streptomycin) in a 5% CO2 incubator overnight at 37°C. Enzymes were neutralized with 10% FBS-DMEM medium. Digested tissue was resuspended in medium and subjected to gravity for 12–15 min and supernatants were subjected four more times to gravity sedimentation. The tumors were digested with cocktail of Collagenase type IV and Hyaluronidase for 30 minutes and CAFs were isolated gravity sedimentation as described above for mammary glands. The MMFs were maintained in DMEM/F-12 media

supplemented with Insulin, Hydrocortisone, epidermal growth factor and 10% FBS (Sigma Aldrich, USA). The fibroblasts isolated from tumors were further enriched by differential trypsinization for two times.

Cell migration and invasion assay—These assays were performed using transwell chambers (Costar, 8.0 mm pore size) as described in our previous study.[35] Briefly, serum starved cells were loaded into the top chamber and bottom chambers contained SFM in the presence or absence of CAFs derived from *f/f;PyT* or *Δ/Δ;PyT* tumors. *Δ/Δ;PyT* CAFs were also provided with rCXCL12. Cells that migrated or invaded across the membrane were counted by fixing in 37% formaldehyde and 25% glutaraldehyde in PBS and stained with 0.1% crystal violet in PBS for 30 minutes. Migrated/invaded cells were detected by light microscopy and high magnification images were captured. Average number of cells migrated per field was calculated.

In vitro transwell vascular permeability and trans-endothelial migration assay

The MEEC vascular permeability was analyzed by utilizing transwell cones (Corning, USA) with 8μM pore size and coated with Matrigel (BD Biosciences, USA) as described before.[36] Briefly, the MEEC (1×10^6 cells) were deposited to the top chamber of matrigel precoated transwells and allowed to adhere for overnight. The MEEC were again seeded for second time as described above. Next day, the fibrobroblasts were co-cultured with MEEC in top chamber. The bottom chamber was provided with culture media added with 3KD FITC-Dextran (Sigma Aldrich). The fluorescence intensity of Dextran diffused to the top chamber was analyzed at different time point and fluorescence intensity was calculated.

For trans-endothelial migration assay, fibroblasts were cultured in the bottom chamber. The upper chamber was seeded with CFSC-tagged MVT1 cells (100,000 cells) and migration of cells across MEEC layer was analyzed in the presence or absence of recombinant CXCL12 (100ng/ml) or AMD3100 (10μM) in the top chamber. The cells were incubated overnight at 37°C and imaged by fluorescence microscope (Leica M165FC and DFC450C camera). The migrated cells were counted manually and data presented as number of cells migrated per field.

Tube formation assay—MEECs were seeded on matrigel coated 24 well plates and incubated at 37°C and 5% CO_2 for 6 hours in the presence or absence of conditioned media (CM) derived from *f/f;PyT* or *Δ/Δ;PyT* CAFs at ratio of 1:4. *f/f;PyT* was also provided with recpmbinant CXCL12 (100ng/ml). High magnification images were captured by light microscope and analyzed by ImageJ using angiogenesis plugin. Average number of mashes formed was calculated as tube formation ability.

Tissue Microarray (TMA)

TMA slides containing paraffin-embedded breast carcinoma tissues were processed at the Pathology Core Facility and Tissue Archives Human Tissue Resource Network at Ohio State University. A total of 460 samples were included in TMA including 10 adjacent normal or non-malignant lesions. IHC on these slides was performed with CXCL12 (1:100, Abcam), CD31 (1:100, Dako) following standard procedure. Level of CXCL12 expression was scored

with Allred score method. Based on Allred scores, 0 and 1 level of CXCL12 expressing samples were grouped as low expression and 1 and 2 level of CXCL12 expressing samples were grouped as high expression samples. $CD31^+$ blood vessels present in a high magnification field were counted manually and samples with ≤ 3 blood vessels were considered as low blood vessel density samples and >3 blood vessels were considered as high blood vessel density samples. Samples were categorized as “Low” when stromal CXCL12 and/or CD31 density was low; samples were categorized as ‘High’ when both stromal CXCL12 and CD31 were high.

Statistical analysis

To study tumor growth and metastatic *in vivo*, more than 10 mice per group were used to detect a 2-fold difference at $\alpha=0.05/2$. All the statistical tests were two-sided. A linear mixed effects model was used to take account of the correlation among observations from the same animal or *in vitro* condition. Two sample t-test was used to compare the groups (Figure. 2 B–C, F–G, and Fig. 3 B–C, E, G–H and Supplementary Figure 4B). Kaplan-Meier analysis was performed to calculate survival rate (Figure. 2A; Figure 4 C–F; Supplementary Figure 8 C–D; 9 A–B, E–F). Statistical testing was performed using ANOVA with Tukey’s-Cramer post testing to identify statistical significance compared to control, setting $p < 0.001$ as the threshold. To test the difference in CXCL12 expression among different stage human breast cancer tissues using TMA, 47 patient samples per group will be needed in order to detect a 30% difference on positive staining, where we assume a 20% vs. 50% positive rate for normal vs. tumors ($\alpha=0.05/2=0.025$ to adjust for two comparisons). Chi square test was used to compare the distribution of CXCL12 and CD31 expression. Pearson’s test was used to analyze the correlation between blood vessel density and CXCL12 expression. All data represent mean ± SEM. A *P* value less than 0.05 was considered statistically significant. *, $p<0.05$; **, $p<0.01$, ***, $p<0.001$ until unless specified.

Supplementary Material

Refer to Web version on PubMed Central for supplementary material.

Acknowledgments

We are thankful to Reham S. Shehab, Sanjit Roy, Chan Fu, Mohamed Adel, and Nitika Agarwal for technical assistance. This work is supported in part by Pelotonia Idea award, Department of Defense level II breakthrough awards, and NIH R01 grants (CA109527 and CA153490) to RKG. DKA was recipient of Pelotonia Postdoctoral award.

References

1. Hennighausen L, Robinson GW. Signaling pathways in mammary gland development. Dev Cell. 2001; 1:467–475. [PubMed: 11703938]
2. Tan J, Buache E, Alpy F, Daguenet E, Tomasetto CL, Ren GS, et al. Stromal matrix metalloproteinase-11 is involved in the mammary gland postnatal development. Oncogene. 2014; 33:4050–4059. [PubMed: 24141782]
3. Nguyen DX, Bos PD, Massague J. Metastasis: from dissemination to organ-specific colonization. Nat Rev Cancer. 2009; 9:274–284. [PubMed: 19308067]
4. Punglia RS, Morrow M, Winer EP, Harris JR. Local therapy and survival in breast cancer. N Engl J Med. 2007; 356:2399–2405. [PubMed: 17554121]

5. Orimo A, Gupta PB, Sgroi DC, Arenzana-Seisdedos F, Delaunay T, Naeem R, et al. Stromal fibroblasts present in invasive human breast carcinomas promote tumor growth and angiogenesis through elevated SDF-1/CXCL12 secretion. Cell. 2005; 121:335–348. [PubMed: 15882617]
6. Muller A, Homey B, Soto H, Ge N, Catron D, Buchanan ME, et al. Involvement of chemokine receptors in breast cancer metastasis. Nature. 2001; 410:50–56. [PubMed: 11242036]
7. Hanahan D, Coussens LM. Accessories to the crime: functions of cells recruited to the tumor microenvironment. Cancer Cell. 2012; 21:309–322. [PubMed: 22439926]
8. Nagasawa T, Hirota S, Tachibana K, Takakura N, Nishikawa S, Kitamura Y, et al. Defects of B-cell lymphopoiesis and bone-marrow myelopoiesis in mice lacking the CXC chemokine PBSF/SDF-1. Nature. 1996; 382:635–638. [PubMed: 8757135]
9. Trimboli AJ, Fukino K, de Bruin A, Wei G, Shen L, Tanner SM, et al. Direct evidence for epithelial-mesenchymal transitions in breast cancer. Cancer Res. 2008; 68:937–945. [PubMed: 18245497]
10. Lin EY, Jones JG, Li P, Zhu L, Whitney KD, Muller WJ, et al. Progression to malignancy in the polyoma middle T oncoprotein mouse breast cancer model provides a reliable model for human diseases. Am J Pathol. 2003; 163:2113–2126. [PubMed: 14578209]
11. Trimboli AJ, Cantemir-Stone CZ, Li F, Wallace JA, Merchant A, Creasap N, et al. Pten in stromal fibroblasts suppresses mammary epithelial tumours. Nature. 2009; 461:1084–1091. [PubMed: 19847259]
12. Egeblad M, Ewald AJ, Askautrud HA, Truitt ML, Welm BE, Bainbridge E, et al. Visualizing stromal cell dynamics in different tumor microenvironments by spinning disk confocal microscopy. Dis Model Mech. 2008; 1:155–167. [PubMed: 19048079]
13. Pei XF, Noble MS, Davoli MA, Rosfjord E, Tilli MT, Furth PA, et al. Explant-cell culture of primary mammary tumors from MMTV-c-Myc transgenic mice. In Vitro Cell Dev Biol Anim. 2004; 40:14–21. [PubMed: 15180438]
14. Takahashi T, Kalka C, Masuda H, Chen D, Silver M, Kearney M, et al. Ischemia- and cytokine-induced mobilization of bone marrow-derived endothelial progenitor cells for neovascularization. Nat Med. 1999; 5:434–438. [PubMed: 10202935]
15. Asahara T, Murohara T, Sullivan A, Silver M, van der Zee R, Li T, et al. Isolation of putative progenitor endothelial cells for angiogenesis. Science. 1997; 275:964–967. [PubMed: 9020076]
16. Taddei A, Giampietro C, Conti A, Orsenigo F, Breviario F, Pirazzoli V, et al. Endothelial adherens junctions control tight junctions by VE-cadherin-mediated upregulation of claudin-5. Nat Cell Biol. 2008; 10:923–934. [PubMed: 18604199]
17. Vandenbroucke E, Mehta D, Minshall R, Malik AB. Regulation of endothelial junctional permeability. Ann N Y Acad Sci. 2008; 1123:134–145. [PubMed: 18375586]
18. Finak G, Bertos N, Pepin F, Sadekova S, Souleimanova M, Zhao H, et al. Stromal gene expression predicts clinical outcome in breast cancer. Nat Med. 2008; 14:518–527. [PubMed: 18438415]
19. Weidner N, Semple JP, Welch WR, Folkman J. Tumor angiogenesis and metastasis–correlation in invasive breast carcinoma. N Engl J Med. 1991; 324:1–8.
20. Weidner N, Folkman J, Pozza F, Bevilacqua P, Allred EN, Moore DH, et al. Tumor angiogenesis: a new significant and independent prognostic indicator in early-stage breast carcinoma. J Natl Cancer Inst. 1992; 84:1875–1887. [PubMed: 1281237]
21. Ivins S, Chappell J, Vernay B, Suntharalingham J, Martineau A, Mohun TJ, et al. The CXCL12/CXCR4 Axis Plays a Critical Role in Coronary Artery Development. Dev Cell. 2015; 33:455–468. [PubMed: 26017770]
22. Li B, Bai W, Sun P, Zhou B, Hu B, Ying J. The effect of CXCL12 on endothelial progenitor cells: potential target for angiogenesis in intracerebral hemorrhage. J Interferon Cytokine Res. 2015; 35:23–31. [PubMed: 24955809]
23. Xu X, Zhu F, Zhang M, Zeng D, Luo D, Liu G, et al. Stromal cell-derived factor-1 enhances wound healing through recruiting bone marrow-derived mesenchymal stem cells to the wound area and promoting neovascularization. Cells Tissues Organs. 2013; 197:103–113. [PubMed: 23207453]
24. Hillmer RE, Boisvert JP, Cucciare MJ, Dwinell MB, Joksimovic M. Generation and characterization of mice harboring a conditional CXCL12 allele. Int J Dev Biol. 2015; 59:205–209. [PubMed: 26505253]

25. Petit I, Jin D, Rafii S. The SDF-1-CXCR4 signaling pathway: a molecular hub modulating neo-angiogenesis. Trends Immunol. 2007; 28:299–307. [PubMed: 17560169]
26. Smolkova B, Mego M, Horvathova Kajabova V, Cierna Z, Danihel L, Sedlackova T, et al. Expression of SOCS1 and CXCL12 Proteins in Primary Breast Cancer Are Associated with Presence of Circulating Tumor Cells in Peripheral Blood. Transl Oncol. 2016; 9:184–190. [PubMed: 27267835]
27. Wallez Y, Huber P. Endothelial adherens and tight junctions in vascular homeostasis, inflammation and angiogenesis. Biochim Biophys Acta. 2008; 1778:794–809. [PubMed: 17961505]
28. Yu PF, Huang Y, Xu CL, Lin LY, Han YY, Sun WH, et al. Downregulation of CXCL12 in mesenchymal stromal cells by TGFbeta promotes breast cancer metastasis. Oncogene. 2017; 36:840–849. [PubMed: 27669436]
29. Tang D, Kang R, Cheh CW, Livesey KM, Liang X, Schapiro NE, et al. HMGB1 release and redox regulates autophagy and apoptosis in cancer cells. Oncogene. 2010; 29:5299–5310. [PubMed: 20622903]
30. Schiraldi M, Raucci A, Munoz LM, Livoti E, Celona B, Venereau E, et al. HMGB1 promotes recruitment of inflammatory cells to damaged tissues by forming a complex with CXCL12 and signaling via CXCR4. J Exp Med. 2012; 209:551–563. [PubMed: 22370717]
31. Feig C, Jones JO, Kraman M, Wells RJ, Deonarine A, Chan DS, et al. Targeting CXCL12 from FAP-expressing carcinoma-associated fibroblasts synergizes with anti-PD-L1 immunotherapy in pancreatic cancer. Proc Natl Acad Sci U S A. 2013; 110:20212–20217. [PubMed: 24277834]
32. Nasser MW, Qamri Z, Deol YS, Ravi J, Powell CA, Trikha P, et al. S100A7 enhances mammary tumorigenesis through upregulation of inflammatory pathways. Cancer research. 2012; 72:604–615. [PubMed: 22158945]
33. McLean AC, Valenzuela N, Fai S, Bennett SA. Performing vaginal lavage, crystal violet staining, and vaginal cytological evaluation for mouse estrous cycle staging identification. J Vis Exp. 2012:e4389. [PubMed: 23007862]
34. Soule HD, McGrath CM. A simplified method for passage and long-term growth of human mammary epithelial cells. In Vitro Cell Dev Biol. 1986; 22:6–12. [PubMed: 2418007]
35. Nasser MW, Wani NA, Ahirwar DK, Powell CA, Ravi J, Elbaz M, et al. RAGE mediates S100A7-induced breast cancer growth and metastasis by modulating the tumor microenvironment. Cancer research. 2015; 75:974–985. [PubMed: 25572331]
36. Martins-Green M, Petreaca M, Yao M. An assay system for in vitro detection of permeability in human “endothelium”. Methods Enzymol. 2008; 443:137–153. [PubMed: 18772015]

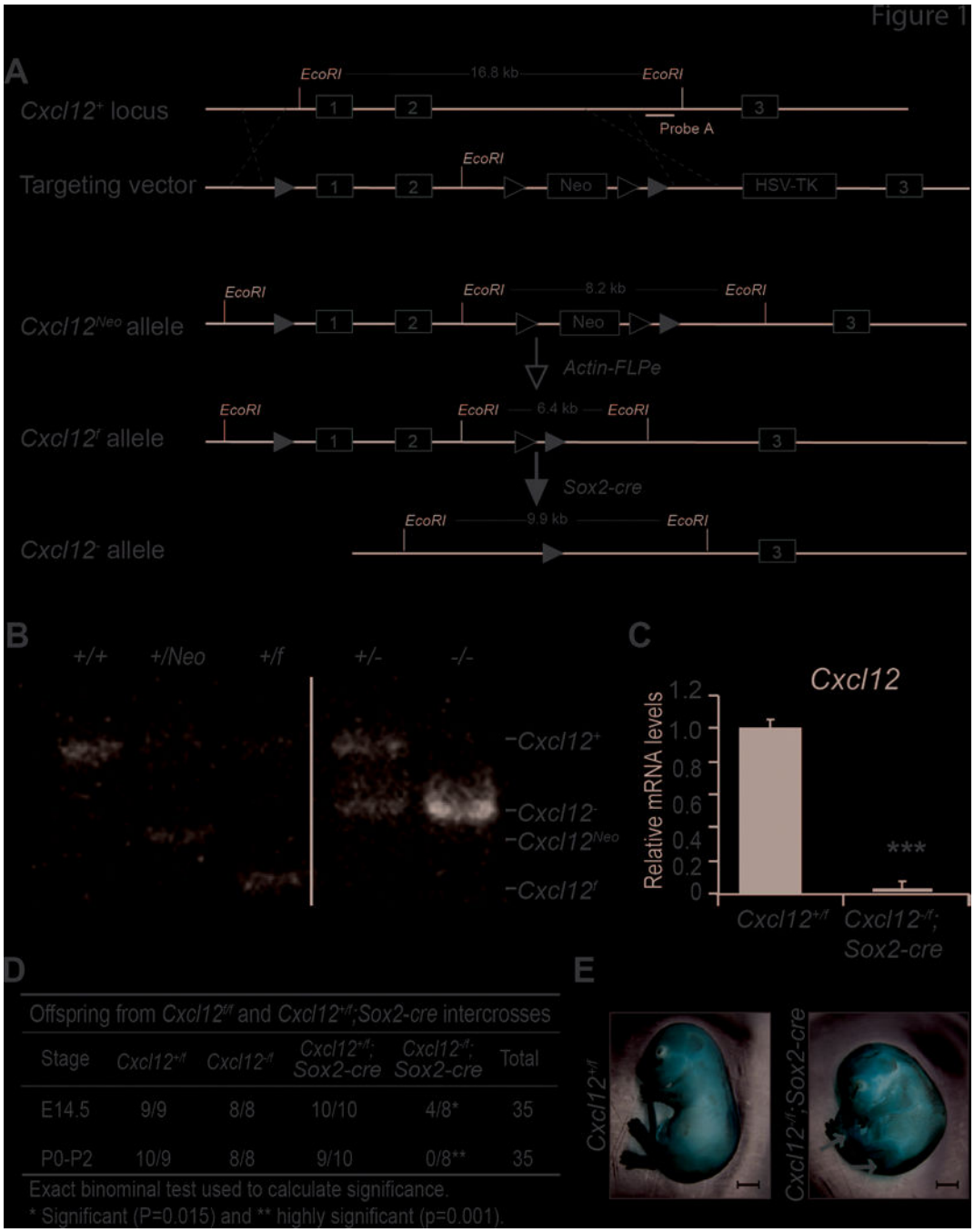

Figure 1. Genetic ablation of *Cxcl12* results in perinatal lethality

(A) Diagram of the *Cxcl12* gene inactivation strategy. Exons are in gray boxes. Targeting vector, exons 1 and 2 were flanked by *LoxP* sequences (black triangles), the neomycin resistance cassette (*Neo*) was flanked by *Frt* sequences (white triangles) and the herpes simplex virus thymidine kinase cassette (HSV-TK) was included for negative selection. $Cxcl12^{Neo}$, targeted allele following homologous recombination in ES cells. $Cxcl12^{f}$, targeted allele following *Actin-FLPe* mediated recombination.

(B) Southern blot; genomic tail DNA was digested with *EcoRI* and hybridized with Probe A.

(C) *Cxcl12* mRNA levels relative to 18s-ribosomal RNA; control $Cxcl12^{+/f}$ samples were normalized to 1.0. ***, p<0.001; two sample t-test.

(D) Genotypes of live offspring from $Cxcl12^{f/f}$ and $Cxcl12^{+/f}$;*Sox2-cre* intercrosses. The number of $Cxcl12^{f/+}$, $Cxcl12^{+/-}$, $Cxcl12^{f/f}$, $Cxcl12^{-/-}$ mice observed/expected are noted for embryos harvested at E14.5 and at birth to 2 days after birth (P0-P2).

(E) Representative pictures of E14.5 embryos. Scale bar, 1mm; arrows indicate hemorrhagic areas.

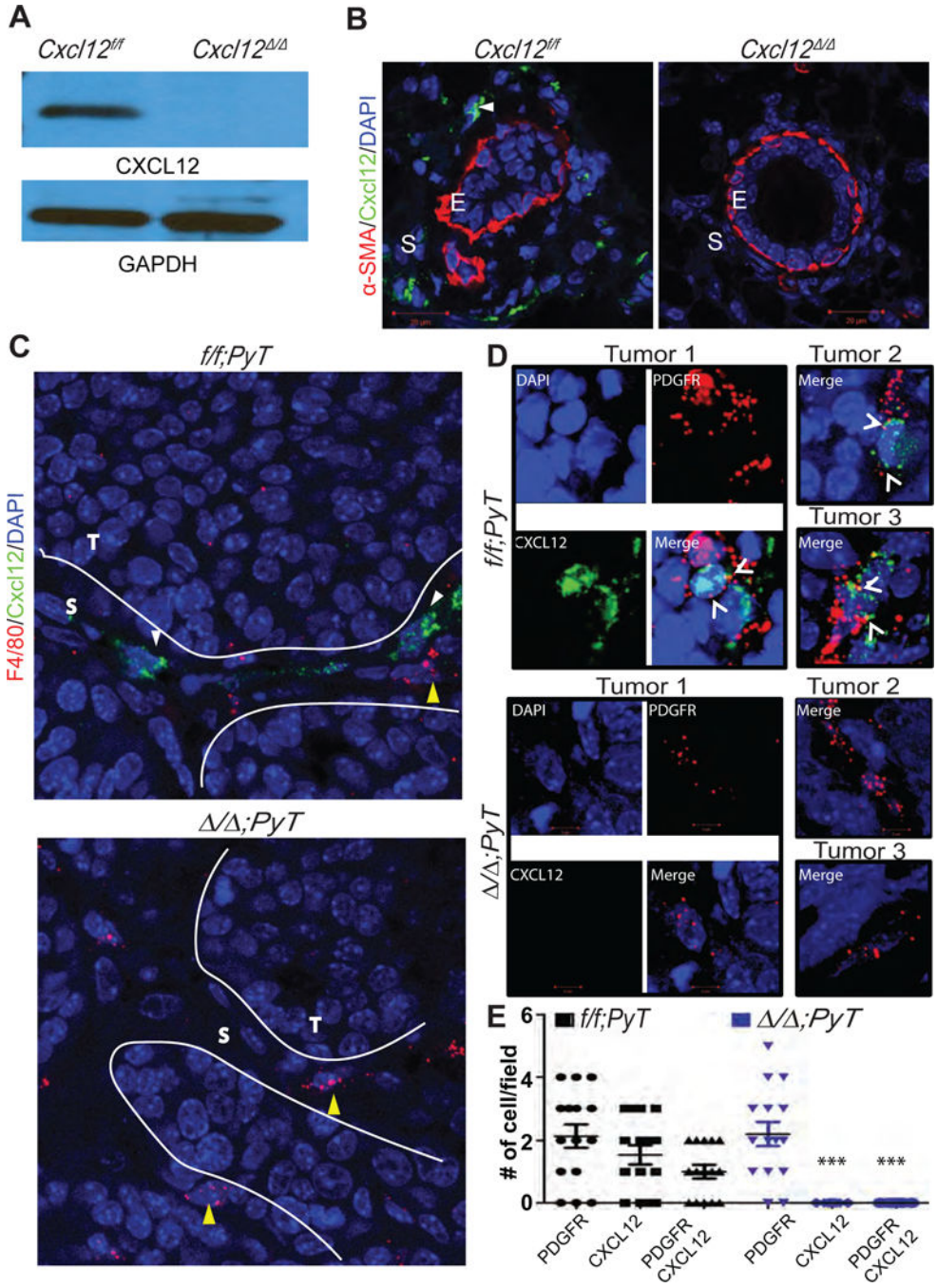

Figure 2. Analysis of fibroblasts-specific CXCL12 in normal mammary and *PyT*tumors

(A) Protein lysates derived from *Cxcl12f/f* or *Cxcl12f/f;Fsp-cre* (*Cxcl12Δ/Δ*) mouse mammary gland fibroblasts (MMFs) were analyzed for CXCL12 by western blot.

(B) Mammary gland sections were immunostained with CXCL12- and αSMA-specific antibodies and analyzed by IF. Dapi was used to counterstain nuclei. Scale bar, 20μm. E, epithelium; S, stromal compartment. Arrow points CXCL12 secreting stromal fibroblasts.

(C) RNA hybridization analysis of tumor sections derived from *f/f;PyT* and *Δ/Δ;PyT* mice. T, tumor cells; S, stroma. Scale bar 20μm.

(D) RNA hybridization analysis of PyT tumor sections using CXCL12 and PDGFRα specific probes. Z-stack images were captured at 63× magnification and 2.5× zoom. Arrowhead points cell double positive for CXCL12 and PDGFR-α mRNA.
(E) Quantification of stained cells per 40× magnification field of tissue sections from (A). N= 15 each group, 5 random fields from 3 different tumors. ***, p <0.001 (comparison of CXCL12 or CXCL12/PDGFR-positive cells between *f/f;PyT* and *Δ/Δ;PyT groups*); two sample t-test.

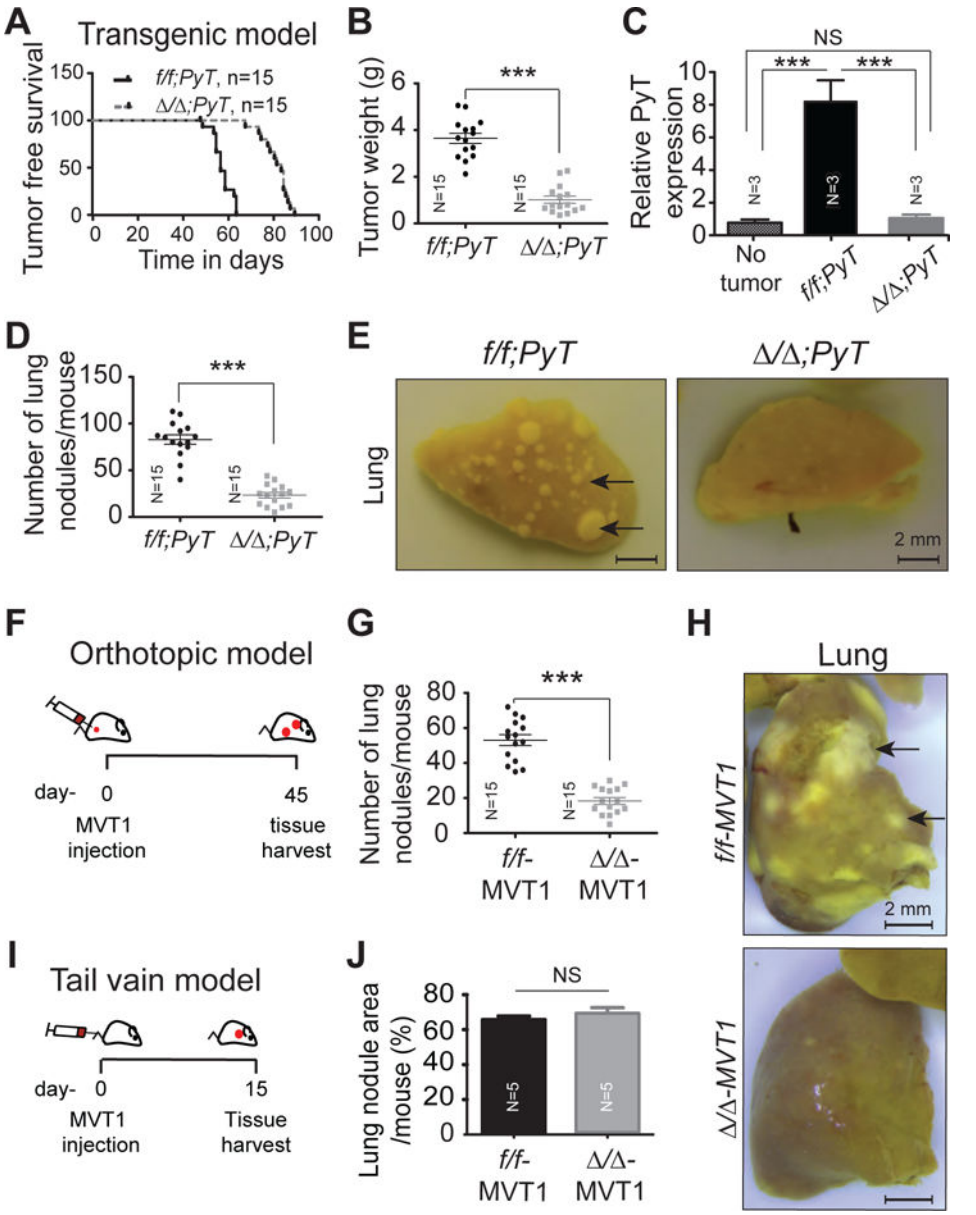

Figure 3. Fibroblast-specific deletion of *Cxcl12* inhibits mammary tumor growth and metastasis. A-D

(A) The *f/f;PyT* (57 days) and *Δ/Δ;PyT* (84 days) mice were observed for time to tumor onset. Log rank t-test; p, <0.0001 (N=15 mice each group).

(B) Weight of tumors harvested from (A).

(C) mRNA was isolated from heart blood collected from wild type mice (no tumor) or primary tumor size matched *f/f;PyT* and *Δ/Δ;PyT* mice and analyzed by RT-qPCR for *PyT* expression normalized to *18s* expression as an indicator of circulatory tumor cells. N=3 mice each group.

(D) Number of metastatic lung nodules in *f/f;PyT* and *Δ/Δ;PyT* mice matched for tumor size

(E) Representative pictures of lungs from (D).

(F) Orthotopic tumor model. *Cxcl12*$^{f/f}$ (f/f-MVT1) and *Cxcl12*$^{\Delta/\Delta}$ (Δ/Δ-MVT1) mice were injected with MVT-1 mammary tumor cells (1×10^6) to the mammary fat pads.
(G) Microscopic quantification of metastatic nodules present on harvested lungs from F.
(H) Representative pictures of lungs harvested from (F).
(I) Tail vein tumor model. MVT1 cells (1×10^6) were injected into the tail vein of *f/f*-MVT1 and *Δ/Δ*-MVT1 mice (N=8 for each group).
(J) H&E stained sections of lungs were analyzed using ImageJ software and the metastatic nodule area (pixels) is presented as a percentage of the total surface lung area (pixels).
NS, non-significant; ***, $p<0.001$.

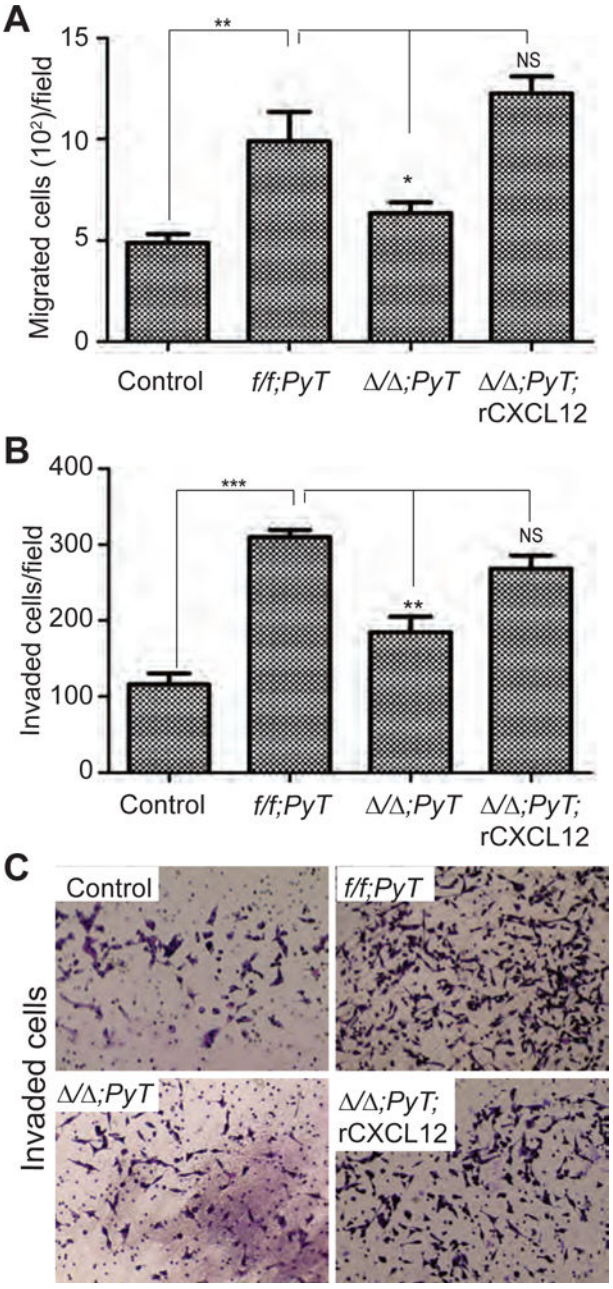

Figure 4. Effect of CAFs-derived CXCL12 on tumor cell migration and matrigel invasion

(A) The migration of MVT-1 cells was analyzed by using transwell migration assay in the presence or absence of *f/f;PyT* CAFs or *Δ/Δ;PyT* CAFs or *Δ/Δ;PyT* CAFs + recombinant CXCL12 (rCXCL12) and the number of cells migrated/field was presented.

(B) The invasion potential of MVT-1 cells was analyzed by using matrigel coated transwell invasion assay in the presence or absence of *f/f;PyT* CAFs or *Δ/Δ;PyT* CAFs or *Δ/Δ;PyT* CAFs + rCXCL12 and the number of cells invaded/field was presented.

(C) The representative images of MVT-1 cells invaded in matrigel coated transwell invasion assay from (B).

Student's t-test was used to compare the groups. * <0.05, ** <0.01, ***<0.001.

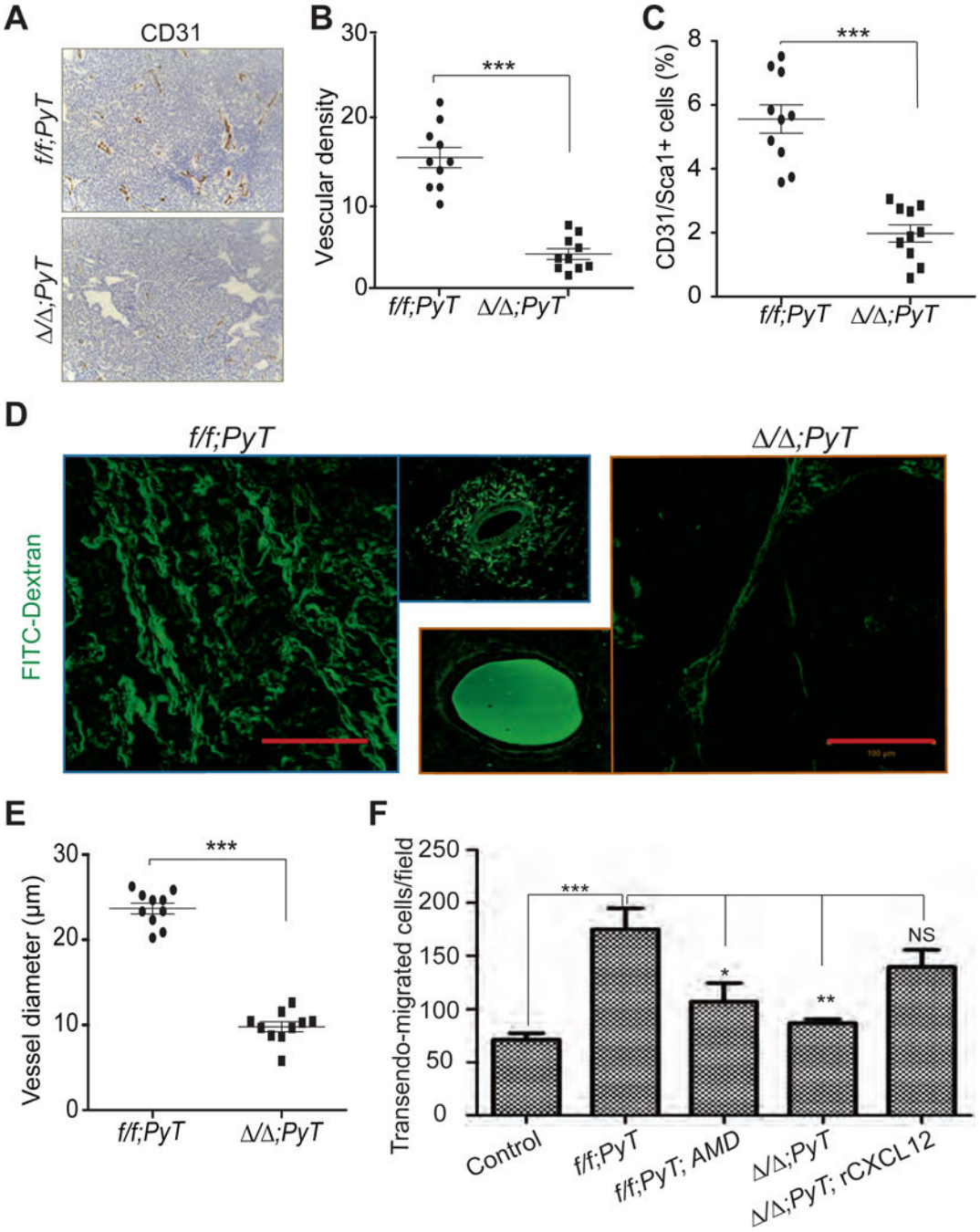

Figure 5. Stromal CXCL12 regulates angiogenesis and blood vessel permeability

(A) Representative pictures of *f/f;PyT* and *Δ/Δ;PyT* tumor sections stained with endothelial cell-specific CD31 antibody. Scale bar, 100μm.

(B) Quantification of vascular density in tumors as determined by the number of $CD31^{+}$ blood vessels (from A) per 20× field.

(C) Quantification of CD31+/Sca1+ cells in tumors as determined by flow cytometry.

(D) Confocal images of tumors from mice injected with Fluorescent-dextran (F-dextran; 2000KD, FITC conjugated). Scale bar, 100μm. Side panels represent higher magnification of single blood vessels. Scale bar 50μm.

(E) Quantification of mean blood vessel diameter determined from images in (D).

(F) The trans-edothelial migration of MVT-1 cells was analyzed by using matrigel coated transwells and MEECs in the presence or absence of CAFs isolated from *f/f;PyT* and *Δ/Δ;PyT* tumors. The trsanswells with *f/f;PyT* and *Δ/Δ;PyT* were treated with AMD-3100 (AMD) and recombinant CXCL12 (rCXCL12) respectively. *, $p<0.05$; **, $p<0.01$; ***, $p<0.001$. One-way anova t-test.

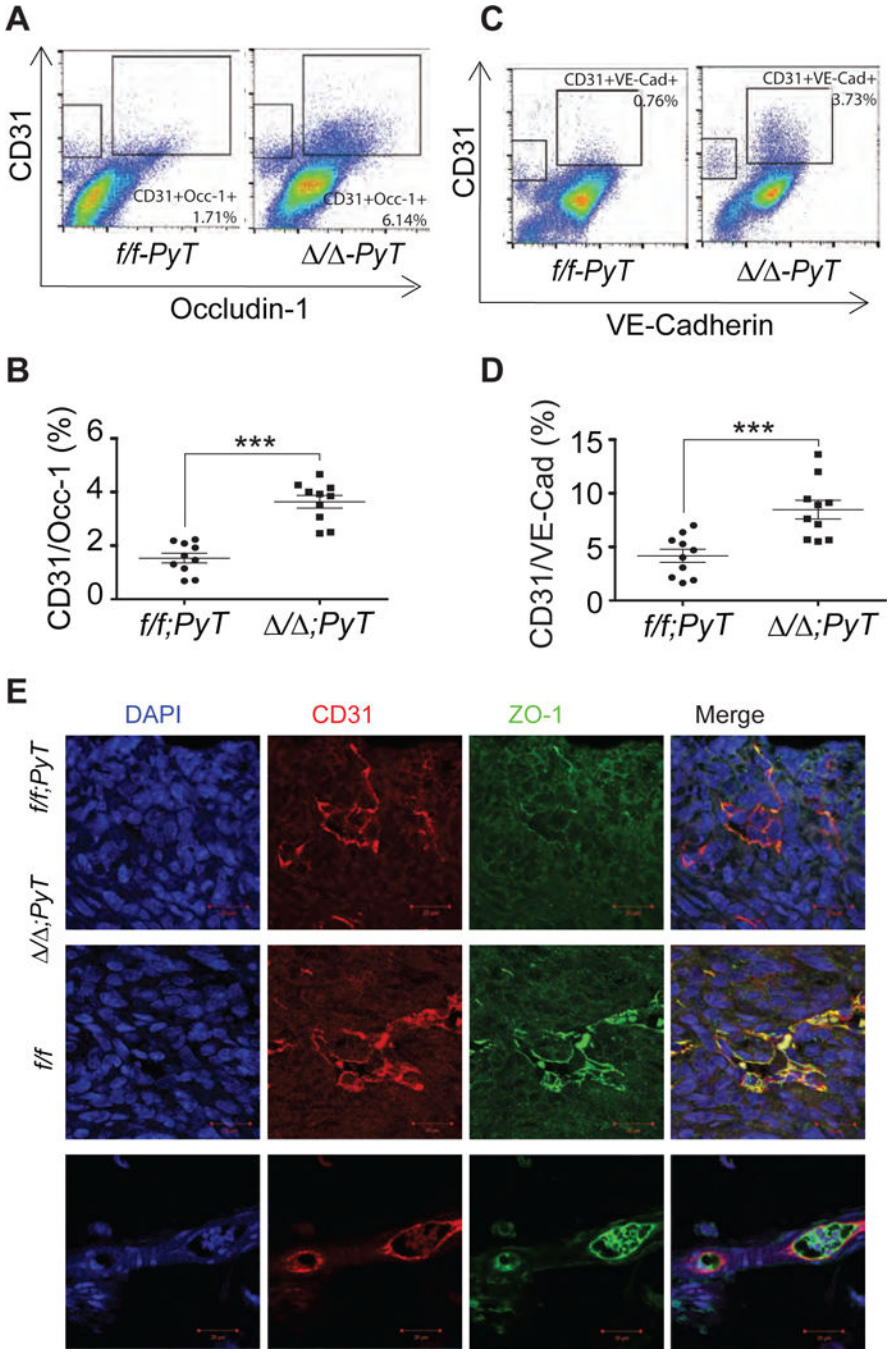

Figure 6. Fibroblast-specific CXCL12 regulates endothelial cell tight junction and adherence molecule expression

(A and C) Flow cytometry analysis of single cell suspension of primary tumors collected from mice of indicated genotypes double stained with CD31 and tight junction molecules Occludine-1 or VE-Cadherin respectively.

(B and D) Quantification of CD31 positive and Occludine-1 (Occ-1) or VE- Cadherin (VE-Cad) positive cells from A and C respectively. ***, $p<0.001$.

(E) Tumor and normal mammary gland (no tumor) sections immunostained with CD31 and ZO-1 specific antibodies and analyzed by IF.

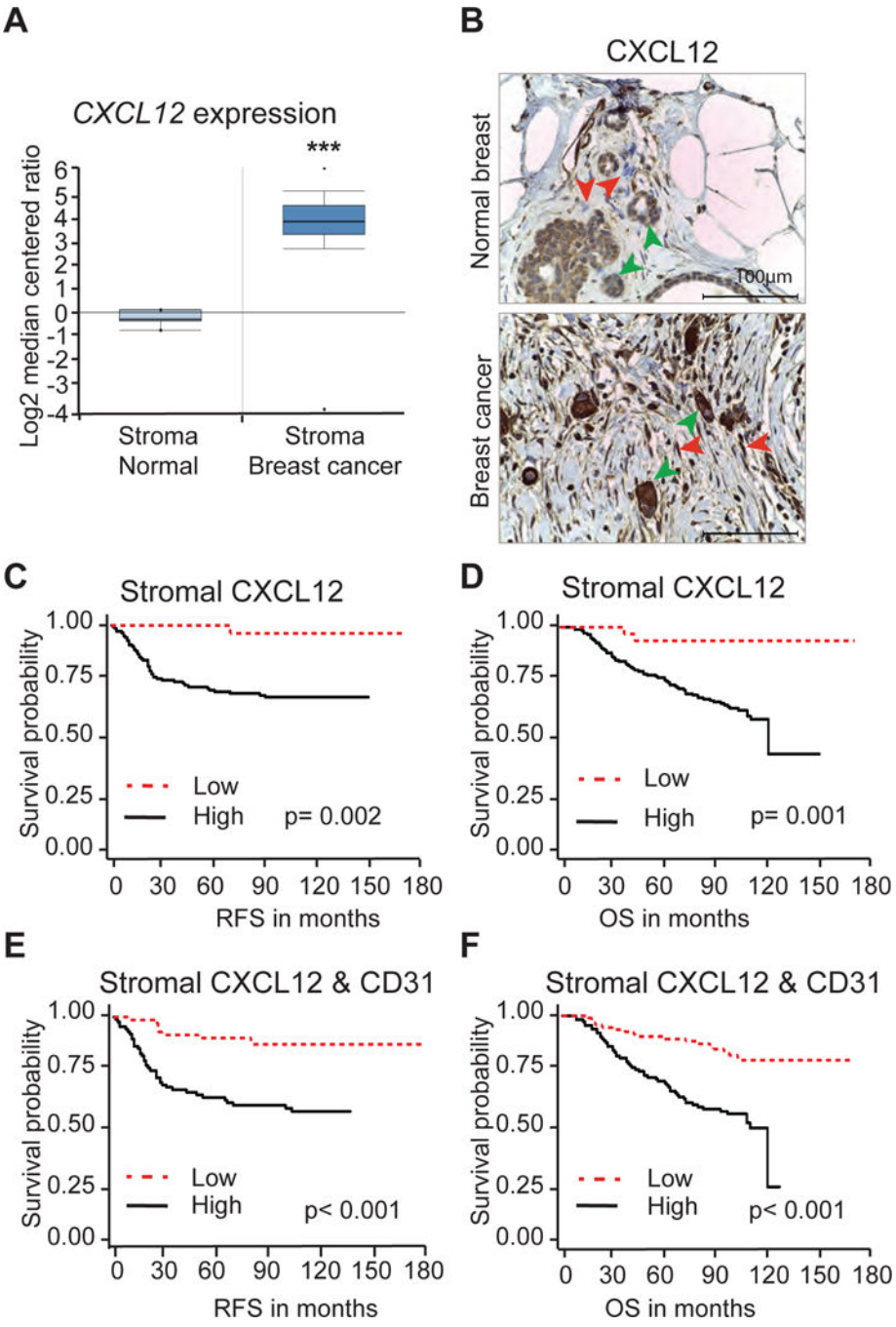

Figure 7. CXCL12 expression levels in stromal fibroblasts predict breast cancer patient survival

(A) *CXCL12* expression in laser-captured microdissected (LCM) breast tumor stroma (53 samples) and adjacent normal stroma (6 samples) derived from *Finak et al.* ***, p<0.001.

(B) IHC analysis of a human Tissue Microarray immunostained with CXCL12 specific antibody. Red arrows point to stromal fibroblasts and green arrows point tumor cells expressing CXCL12.

(C and D) Recurrence Free Survival (RFS) and Overall Survival (OS) of breast cancer patients expressing high or low CXCL12 in stromal fibroblasts.

(E and F) RFS and OS of breast cancer patients expressing high or low CXCL12 and CD31.